# Aggregate Harmonic Fingerprint Models of PV Inverters. Part 1: Operation at Different Powers

X. Xu, A. Collin, S. Djokic
The University of Edinburgh
Edinburgh, Scotland, UK

S. Müller and J. Meyer
TU Dresden
Dresden, Germany

J. Myrzik
TU Dortmund
Dortmund, Germany

R. Langella and A. Testa
The University of Campania
Aversa, Italy

***Abstract*—This paper is the first part of a two-part series on the development of aggregate frequency domain models of PV inverters (PVIs). The developed PVI models are expressed in the form of harmonic admittance matrix (HAM) of a coupled Norton model, also known as the harmonic fingerprint model (HFM). The development of accurate measurement-based HFMs requires considerable amount of measurements, which further increase in case of PVIs, as they typically exhibit strong power-dependent changes in harmonic emission. The authors propose a novel approach, which significantly reduces the number of measurements, as it requires only two sets of measurements at a single operating power: one with the fundamental voltage component, and another with individual voltage harmonics added one by one to the fundamental component. These two sets of measurements are used to calculate a "reference HAM", which is then multiplied by two coefficients calculated from the power-dependent changes of the PVIs total subgroup current harmonic distortion, $THDS_I$. The presented methodology is illustrated and validated using a comprehensive laboratory tests with three different PVIs and it can be easily applied to other types of power electronic devices with similar characteristics.**

***Index Terms*—Frequency-domain, harmonic fingerprint model, harmonics, photovoltaic inverter, power quality.**

## I. Introduction

Due to a range of economic incentives, policy support, technology improvements and reduced costs, the number of photovoltaic inverters (PVIs) is continuously increasing, particularly in terms of small PVI units connected to the residential low voltage (LV) networks. PVIs are nonlinear power electronic devices characterized by an inherent harmonic emission, which typically changes with operating power and is additionally affected by the presence of supply voltage waveform distortions (e.g. [1-3]). Consequently, the analysis of harmonic interactions between the individual PVIs, between the PVIs and supplying grid and between the PVIs and other connected loads is becoming an increasingly complex task, as it involves modelling of a large number of nonlinear power electronic devices. Nevertheless, the accurate models of PVIs, capable of correctly representing their harmonic emission characteristics under the entire range of operating powers and for different voltage supply conditions, are crucial for evaluating possible negative impact of a large number of PV inverters in LV and medium voltage networks.

The two most common harmonic modelling approaches are use of component based models (CBMs) and frequency domain model (FDMs). Development of a CBM for a PVI requires *a priori* knowledge of the inverter circuit topology and applied control schemes, which are usually difficult to obtain from the manufacturer, or to identify by inspecting the PVI circuits [4]. On the other hand, measurement-based FDMs do not require knowledge on the exact circuit topologies and control algorithms, but usually require a large number of measurements to correctly represent impact of supply voltage harmonics on the emission of current harmonics of modelled equipment. One of the commonly used FDMs is expressed in the form of harmonic admittance matrix (HAM) of a coupled Norton model, also known as the harmonic fingerprint model (HFM), [5]. (Note: Generally, terms "HAM" and "HFM are interchangeable; but in this paper the term HAM is used either to denote the matrix elements, or to refer to the HFM matrix itself.) The PVIs typically exhibit strong power-dependent changes of harmonic characteristics and a number of different HFMs should be obtained for different operating powers, resulting in a further increase of the required measurements.

This paper, which is the first part of a two-part series on the development of aggregate HFMs of PVIs, presents a novel modelling approach, which significantly reduces number of required measurements for HFM development, as it requires only two sets of measurements at a single PVI operating power. These two sets of measurements are used to calculate a "reference HAM", which is then multiplied by the two coefficients calculated from the power-dependent changes of PVIs total subgroup current harmonic distortion, $THDS_I$. The analysis in the paper is illustrated and validated using a comprehensive laboratory tests with three different PVIs.

## II. Development of HAM-Based FDMs for PVIs

The simplest FDM is a "constant current source" model, in which each current harmonic is represented by one current source with constant magnitude and phase angle, determined in measurements with ideally sinusoidal supply voltage. When presence of voltage distortion influences changes in harmonic emission of modelled equipment, a more accurate "Norton FDM" is obtained in additional measurements, describing the dependency of current harmonics on the same-order supply voltage harmonics by an admittance connected in parallel to the corresponding current source for each harmonic order.

To include dependencies between the voltage and current harmonics of different orders (i.e. "harmonic couplings"), a "coupled Norton FDM" is used (e.g. [6]), in which HAM describes how each current harmonic is influenced by all voltage harmonics. However, when the modelled equipment exhibits distinctive power-dependent changes of harmonic characteristics, further measurements are required for deriving additional HFMs, in order to ensure that appropriate HFMs are used for the entire range of equipment operating powers. The development of measurement-based HFMs is discussed next, in order to introduce a suitable form of HAM, which is then used in a proposed approach aimed at significantly reducing the number of required measurements.

### *A. Analytical (HAM) Formulation of HFM*

A general form of HFM, in which HAM represents various relationships between fundamental and harmonic components of supply voltage and equipment current, can be written as:

$$\begin{bmatrix}\bar{I}^1\\ \bar{I}^2\\ \bar{I}^3\\ \vdots\\ \bar{I}^n\end{bmatrix}=\begin{bmatrix}\bar{Y}^{1,1} & \bar{Y}^{1,2} & \bar{Y}^{1,3} & \dots & \bar{Y}^{1,n}\\ \bar{Y}^{2,1} & \bar{Y}^{2,2} & \bar{Y}^{2,3} & \dots & \bar{Y}^{2,n}\\ \bar{Y}^{3,1} & \bar{Y}^{3,2} & \bar{Y}^{3,3} & \dots & \bar{Y}^{3,n}\\ \vdots & \vdots & \vdots & \ddots & \vdots\\ \bar{Y}^{n,1} & \bar{Y}^{n,2} & \bar{Y}^{n,3} & \dots & \bar{Y}^{n,n}\end{bmatrix}\times\begin{bmatrix}\bar{V}^1\\ \bar{V}^2\\ \bar{V}^3\\ \vdots\\ \bar{V}^n\end{bmatrix} \quad (1)$$

where: $\bar{I}^h$, $\bar{V}^H$ denote fundamental and harmonic components of equipment input ac current, and fundamental and harmonic components of ac supply voltage, respectively, for $h$, $H$ = 1, 2, …, $n$, where $n$ is the maximum considered harmonic order (19 in this paper). All mutual dependencies are represented by HAM elements, $\bar{Y}^{h,H}$, with Fig. 1 illustrating the four related HAM parts. Part 1 is one admittance, $\bar{Y}^{1,1}$, representing impact of fundamental voltage $\bar{V}^1$ on one part of the total fundamental current, $\bar{I}_A^1$. Part 2 is a column-matrix $\bar{\boldsymbol{Y}}^{\boldsymbol{h},\boldsymbol{1}}$, representing impact of fundamental voltage $\bar{V}^1$ on one part of the total harmonic currents of all considered orders, $\bar{\boldsymbol{I}}_{\boldsymbol{A}}^{\boldsymbol{h}}$. Part 3 is a row-matrix $\bar{\boldsymbol{Y}}^{\boldsymbol{1},\boldsymbol{H}'}$, for $H'$ = 2, …, $n$, representing impact of all voltage harmonics, $\bar{\boldsymbol{V}}^{\boldsymbol{H}'}$**,** on the second part of the total fundamental current, $\bar{I}_B^1$. Part 4 is a matrix, $\bar{\boldsymbol{Y}}^{\boldsymbol{h},\boldsymbol{H}'}$, representing impact of all voltage harmonics $\bar{\boldsymbol{V}}^{\boldsymbol{H}'}$ on the second part of the total harmonic currents of all considered orders, $\bar{\boldsymbol{I}}_{\boldsymbol{B}}^{\boldsymbol{h}}$.

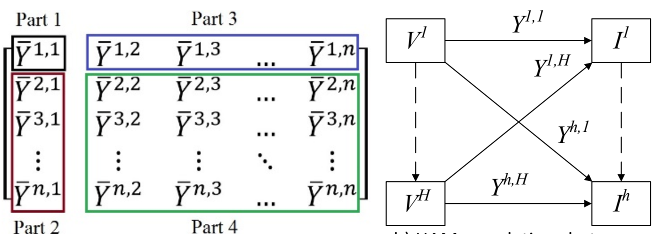


a) four different parts of HAM b) HAM correlations between voltage and current harmonics

Fig. 1. Dependencies between voltage and current harmonics in HAM.

The following matrix formulation is used as a basis for the modified HFM presented in Section III:

$$\bar{\boldsymbol{I}}^{\boldsymbol{h}}=\bar{\boldsymbol{Y}}^{\boldsymbol{h},\boldsymbol{H}}\times\bar{\boldsymbol{V}}^{\boldsymbol{H}}=\bar{\boldsymbol{Y}}^{\boldsymbol{h},\boldsymbol{1}}\times\bar{V}^1+\bar{\boldsymbol{Y}}^{\boldsymbol{h},\boldsymbol{H}'}\times\bar{\boldsymbol{V}}^{\boldsymbol{H}'}=\bar{\boldsymbol{I}}_{\boldsymbol{A}}^{\boldsymbol{h}}+\bar{\boldsymbol{I}}_{\boldsymbol{B}}^{\boldsymbol{h}}=\bar{\boldsymbol{I}}_{\boldsymbol{Tot}}^{\boldsymbol{h}} \quad (2)$$

Equations (1)-(2) can be normalized, if corresponding quantities are divided by the fundamental component of supply voltage and total fundamental component of equipment current. For example, elements $\bar{Y}^{h,H}$ of HAM are normalized into $\bar{Y}_{\%}^{h,H}$ elements of HAM$_{\%}$ as:

$$\bar{\boldsymbol{Y}}^{h,H}=\frac{\bar{I}_{Tot}^h}{\bar{V}^H}=\frac{\bar{I}_{\%}^h}{\bar{V}_{\%}^H}\times\frac{\bar{I}_{Tot}^1}{\bar{V}^1}=\bar{\boldsymbol{Y}}_{\%}^{h,H}\times\frac{\bar{I}_{Tot}^1}{\bar{V}^1} \quad (3)$$

allowing to separate impact of fundamental voltage (Parts 1 and 2 of HAM) from the impact of voltage harmonics (Parts 3 and 4 of HAM) on the corresponding parts of fundamental and harmonic currents, indicated by subscripts A and B:

$$\bar{\boldsymbol{I}}_{\%\_\boldsymbol{A}}=\begin{bmatrix}\bar{I}_{\%\_A}^1\\ \bar{I}_{\%\_A}^2\\ \bar{I}_{\%\_A}^3\\ \vdots\\ \bar{I}_{\%\_A}^n\end{bmatrix}=\begin{bmatrix}\bar{Y}_{\%}^{1,1}\\ \bar{Y}_{\%}^{2,1}\\ \bar{Y}_{\%}^{3,1}\\ \vdots\\ \bar{Y}_{\%}^{n,1}\end{bmatrix}\times\bar{V}_{\%}^1 \quad (4)$$

$$\bar{\boldsymbol{I}}_{\%\_\boldsymbol{B}}=\begin{bmatrix}\bar{I}_{\%\_B}^1\\ \bar{I}_{\%\_B}^2\\ \bar{I}_{\%\_B}^3\\ \vdots\\ \bar{I}_{\%\_B}^n\end{bmatrix}=\begin{bmatrix}\bar{Y}_{\%}^{1,2} & \bar{Y}_{\%}^{1,3} & \bar{Y}_{\%}^{1,4} & \dots & \bar{Y}_{\%}^{1,n}\\ \bar{Y}_{\%}^{2,2} & \bar{Y}_{\%}^{2,3} & \bar{Y}_{\%}^{2,4} & \dots & \bar{Y}_{\%}^{2,n}\\ \bar{Y}_{\%}^{3,2} & \bar{Y}_{\%}^{3,3} & \bar{Y}_{\%}^{3,4} & \dots & \bar{Y}_{\%}^{3,n}\\ \vdots & \vdots & \vdots & \ddots & \vdots\\ \bar{Y}_{\%}^{n,2} & \bar{Y}_{\%}^{n,3} & \bar{Y}_{\%}^{n,4} & \dots & \bar{Y}_{\%}^{n,n}\end{bmatrix}\times\begin{bmatrix}\bar{V}_{\%}^2\\ \bar{V}_{\%}^3\\ \bar{V}_{\%}^4\\ \vdots\\ \bar{V}_{\%}^n\end{bmatrix} \quad (5)$$

$$\bar{\boldsymbol{I}}_{\%\_\boldsymbol{Tot}}=\bar{\boldsymbol{I}}_{\%\_\boldsymbol{A}}+\bar{\boldsymbol{I}}_{\%\_\boldsymbol{B}} \quad (6)$$

where: $\bar{\boldsymbol{I}}_{\%_\boldsymbol{A}}$and $\bar{\boldsymbol{I}}_{\%\_\boldsymbol{B}}$ are summed up in $\bar{\boldsymbol{I}}_{\%\_\boldsymbol{Tot}}$ (all as column vectors), to properly model combined effects of fundamental and harmonic components of supply voltage on resulting/total fundamental and harmonic components of equipment current.

### *B. Deriving HAM-Based HFM from Measurements*

Parts 1 and 2 of HAM are obtained in a small number of tests with ideally sinusoidal supply voltage, with fundamental voltage magnitude varied in a range from 0.9 p.u. to 1.1 p.u., by dividing measured fundamental and harmonic currents with the applied fundamental voltage. Calculation of Parts 3 and 4, however, requires a large number of measurements with the considered voltage harmonic orders of different magnitudes and phase angles. As illustrated in [7], a few thousands of different measurement points are typically required, even when only individual harmonics are added one by one to fundamental voltage (limited number of tests with different harmonic combinations is used for HFM validation purposes). Importantly, when equipment changes its harmonic emission characteristics at different operating powers, as is the case for PVIs, one HFM should be obtained for one operating power, resulting in a further increase of the required measurements

The HFM measurements used in this paper are performed for two PVIs operating in the range from 100% of their rated power, $P_{rated}$, down to 10% of $P_{rated}$ with a step of 10% of $P_{rated}$ and for one PVI from 50% to 5% of $P_{rated}$ with a 5% step. The considered voltage harmonic orders are: 2, 4 and 6 (even) and 3, 5, 7, 9, 11, 13, 15, 17 and 19 (odd), with magnitudes varied in the range from 0.1 of the corresponding limits, $V_{h,limit}$, in [8] to 1.2×$V_{h,limit}$, with a step of 0.1$V_{h,limit}$, while harmonic phase angles were varied in the range from 0°-360° in steps of 30°.

In tests with individual harmonics, the rms value of the resultant supply voltage is maintained at 1 p.u. (230 V) and no source impedance was connected (except a small impedance of the connecting cables). Ideally sinusoidal test voltage is denoted as "WF1", while two distorted voltage waveforms with the combinations of harmonics (used for the validation purposes and for the development of a modified HFM presented in Section III) are denoted as "WF2" and "WF3" (derived from actual measurements in LV networks, see [4]).

## *C. Results of Measurement-Based HFMs*

Table I lists basic characteristics of the three tested PVIs, while Figs. 2-4 illustrates how all elements of $HAM_{\%}$ ($|\overline{\boldsymbol{Y}}_{\%}^{h,H}|$) change for a number of selected PVI operating powers.

TABLE I. BASIC DATA OF THE THREE TESTED PVIS

| PV Inverter | PVI-A | PVI-B | PVI-C |
|---|---|---|---|
| **Technology** | Transformerless | HF-transformer | LF transformer |
| **Phase connection** | Single-phase | Three-phase | Single-phase |
| **Rated power (kVA)** | 4.6 | 10 | 4.6 |

The results in Figs. 2-4 show that: a) all PVIs exhibit strong power-dependent changes in harmonic emission, which are most pronounced for PVI-B, b) the values of $HAM_{\%}$ elements increase as PVIs operating powers reduce, and c) the diagonal elements of $HAM_{\%}$ have much higher values than off-diagonal elements for all the three PVIs. It should be noted that the presented results are normalized values, giving PVI harmonic currents in percentage of the fundamental current, not absolute harmonic currents, which are typically, but not always, highest for the PVIs operating at rated powers (for a more detailed analysis and discussion see e.g. [4]).

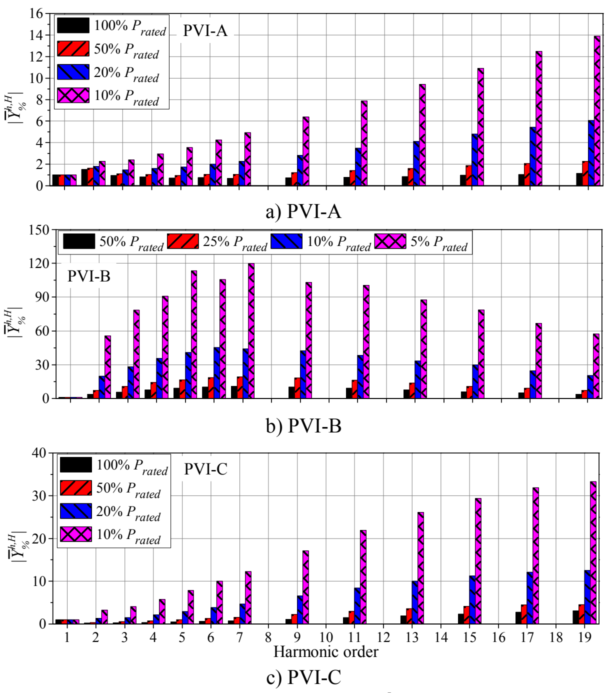


Fig. 2. Power-dependency of diagonal $\overline{\boldsymbol{Y}}_{\%}^{h,H}$ elements of $HAM_{\%}$.

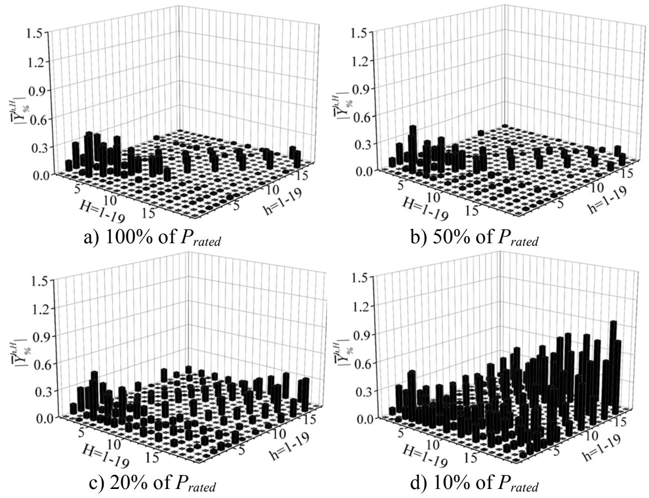


Fig. 3. Power-dependency of off-diagonal $\overline{\boldsymbol{Y}}_{\%}^{h,H}$ elements of $HAM_{\%}$ (PVI-A).

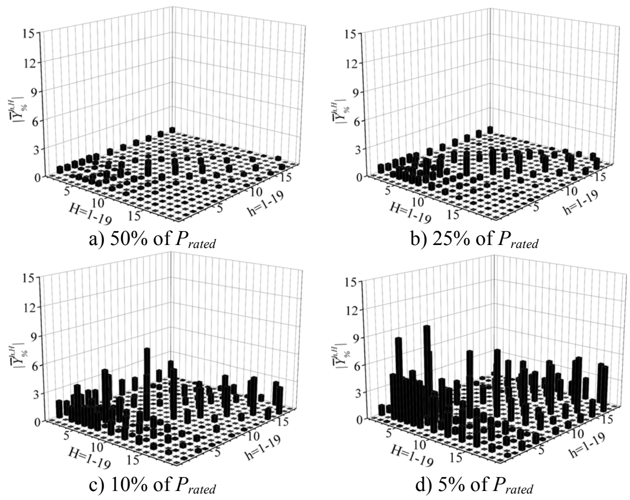


Fig. 4. Power-dependency of off-diagonal $\overline{\boldsymbol{Y}}_{\%}^{h,H}$ elements of $HAM_{\%}$ (PVI-B).

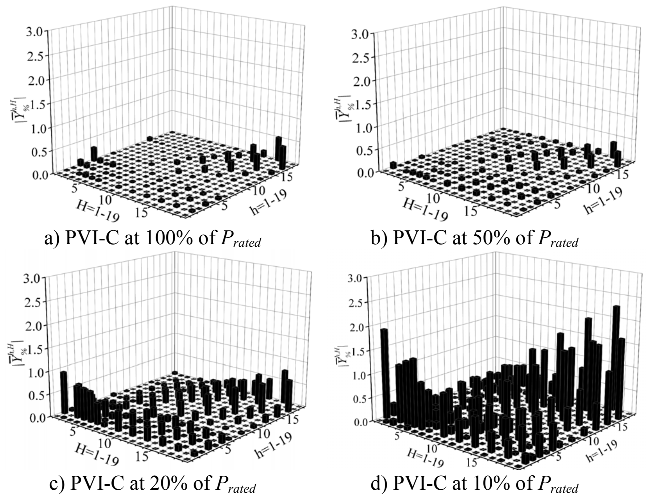


Fig. 5. Power-dependency of off-diagonal $\overline{\boldsymbol{Y}}_{\%}^{h,H}$ elements of $HAM_{\%}$ (PVI-C).

## III. THD-Based Approach for HAM Estimation

The results in Figs. 2-5 demonstrate strong power-dependent changes of harmonic characteristics of tested PVIs. This suggests that it would be necessary to obtain HAMs for PVIs operating at different powers, in order to correctly model their impact on the grid with the corresponding FDMs. For the measurement-based FDMs, this will then require to repeat the testing procedure for each relevant or considered operating power, therefore significantly increasing the total number of measurements. Additionally, related FDMs will be available for only a limited number of selected and in-advance measured operating powers, with each FDM requiring to store a relatively large amount of HAM data (19 x 19 = 361 elements). Effectively, all these aspects of measurement-based HFMs are limiting their practical application, particularly when the aggregate impact of a large number of PVIs should be assessed.

### *A. HAM Modification Using Only PVI Operating Power*

This section presents a suitable modification of the HFM given by (4)-(6), which significantly simplifies representation of power-dependent changes of equipment harmonic emission, as it does not require to derive different measurement-based HAMs for different operating powers of equipment.

The proposed approach assumes that a single set of HFM measurements (one with the fundamental voltage and another with superimposed individual harmonics, as described in Section II.B), is available for equipment operating at a single power level, e.g. at $P_{rated}$. From this single HFM measurement set, the corresponding reference $HAM_{\%\_ref}$ (with elements $\bar{\boldsymbol{Y}}^{\boldsymbol{h,H}}_{\boldsymbol{\%\_ref}}$) can be derived and then two reference values of equipment $THDS_I$ (related to "subgroup concept" defined in [9]) can be calculated from the two current harmonic spectra for $\bar{\boldsymbol{I}}^{\boldsymbol{h}}_{\boldsymbol{ref\_A}}$ and $\bar{\boldsymbol{I}}^{\boldsymbol{h}}_{\boldsymbol{ref\_B}}$: $THDS_{I\_ref\_A}$ and $THDS_{I\_ref\_B}$, respectively.

To obtain $HAM_{\%}(P)$, and in that way HFM($P$), at any other operating power $P$, no further HFM measurements are needed. Instead, two additional tests are required, related to:

1) Measurements of equipment $THDS_I$ values with ideally sinusoidal supply voltage (WF1), in which equipment is adjusted to operate across a full range of powers. This allows to obtain values of $THDS_{I\_WF1}(P)=THDS_{I\_A}(P)$;

2) Measurements of $THDS_I$ values with two typically distorted supply voltage waveforms (WF2 and WF3), again applied to equipment adjusted to operate across its full range of powers. This allows to obtain two corresponding sets of values of $THDS_{I\_WF2}(P)$ and $THDS_{I\_WF3}(P)$, from which values of $THDS_{I\_B}(P)$ at any operating power $P$ are calculated as:

$$THDS_{I\_B}(P) = \left(\frac{THDS_{I\_WF2}(P)+THDS_{I\_WF3}(P)}{2}\right) - THDS_{I\_A}(P) \qquad (7)$$

Afterwards, two coefficients required for modification, $k_{THD\_A}(P)$ and $k_{THD\_B}(P)$, are calculated for a given operating power $P$ from the known values of $THDS_{I\_A}(P)$ and $THDS_{I\_B}(P)$ divided by the values of $THDS_{I\_ref\_A}$ and $THDS_{I\_ref\_B}$, obtained from the reference $HAM_{\%\_ref}$:

$$k_{THD_A}(P) = THDS_{I\_A}(P)/THDS_{I\_ref\_A} \qquad (8)$$

$$k_{THD_B}(P) = THDS_{I\_B}(P)/THDS_{I\_ref\_B} \qquad (9)$$

and elements of the modified $HAM_{\%}(P)$ are calculated from the elements of the reference $HAM_{\%\_ref}$ multiplied by $k_{THD\_A}(P)$ and $k_{THD\_B}(P)$:

$$\bar{\boldsymbol{Y}}^{\boldsymbol{h,1}}_{\%}(P) = k_{THD\_A}(P) \times \bar{\boldsymbol{Y}}^{\boldsymbol{h,1}}_{\boldsymbol{\%\_ref}} \qquad (10)$$

$$\bar{\boldsymbol{Y}}^{\boldsymbol{h,H'}}_{\%}(P) = k_{THD\_B}(P) \times \bar{\boldsymbol{Y}}^{\boldsymbol{h,H'}}_{\boldsymbol{\%\_ref}} \qquad (11)$$

The resulting harmonic current emission at operating power $P$, $\bar{\boldsymbol{I}}^{\boldsymbol{h}}_{\boldsymbol{Tot}}(P)$, for given voltage supply conditions $\bar{\boldsymbol{V}}^{\boldsymbol{H}}$, can be finally obtained as:

$$\bar{\boldsymbol{I}}^{\boldsymbol{h}}_{\boldsymbol{Tot}}(P) = \bar{\boldsymbol{I}}^{\boldsymbol{h}}_{\boldsymbol{A}}(P) + \bar{\boldsymbol{I}}^{\boldsymbol{h}}_{\boldsymbol{B}}(P) = \bar{\boldsymbol{Y}}^{\boldsymbol{h,1}}(P) \times \bar{V}^{\boldsymbol{1}} + \bar{\boldsymbol{Y}}^{\boldsymbol{h,H'}}(P) \times \bar{\boldsymbol{V}}^{\boldsymbol{H'}} \qquad (12)$$

Effectively, the above approach estimates changes in equipment harmonic characteristics at different operating powers using two coefficients proportional to the changes in related $THDS_I$ values to multiply reference $HAM_{\%\_ref}$.

Fig. 6 illustrates the proposed approach, where $HAM_{\%\_ref}$ was available for PVI-A and PVI-C operating at 100% of $P_{rated}$ and for PVI-B operating at 50% of $P_{rated}$.

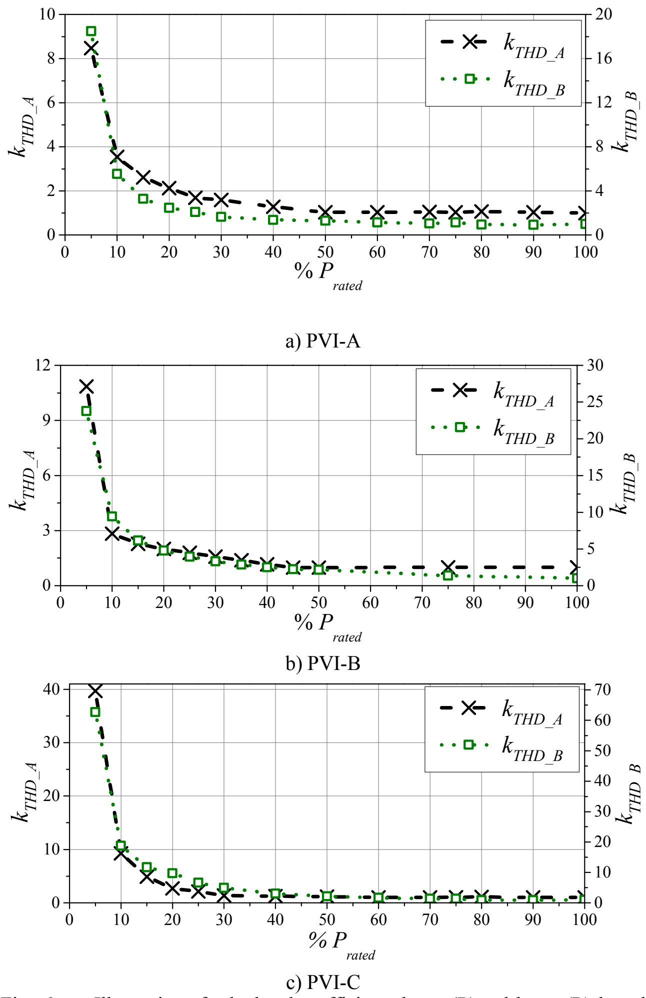


Fig. 6. Illustration of calculated coefficients $k_{THD\_A}(P)$ and $k_{THD\_B}(P)$, based on power-dependent changes of $THDS_{I\_A}(P)$ and $THDS_{I\_B}(P)$, respectively.

In order to assess the accuracy of the proposed approach, the estimated values of $HAM_{\%\_est}(P)$ elements, $\bar{\boldsymbol{Y}}^{\boldsymbol{h,H}}_{\boldsymbol{\%\_est}}(P)$, are compared with the values obtained in measurements, i.e. with $HAM_{\%\_meas}(P)$ calculated from a full set of HFM measurements at each considered operating power $P$, giving corresponding elements $\bar{\boldsymbol{Y}}^{\boldsymbol{h,H}}_{\boldsymbol{\%\_meas}}(P)$. Fig. 7 illustrates that 95th percentile values of relative differences between the elements of two corresponding $HAM_{\%}$ pairs (estimated vs measured) for all three PVIs and for the entire range of their operating powers are small. These values are obtained as:

$$DIFF_{95^{th}}(P) = \left(\frac{|\bar{Y}^{h,H}_{\%est}(P) - \bar{Y}^{h,H}_{\%meas}(P)|}{\sum_{H=1}^{n}\sum_{h=1}^{n}|\bar{Y}^{h,H}_{\%meas}(P)|}\right)_{95^{th}} \times 100\% \quad (13)$$

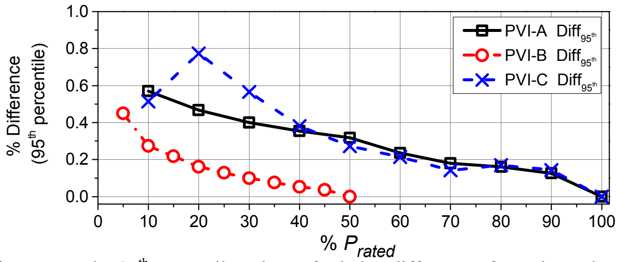


Fig. 7. The 95th percentile values of relative differences for estimated and measured $HAM_{\%}(P)$ elements (modification using only PVI operating power).

### *B. HAM Modification Using Actual $THDS_I$ Values at Specific PVI Operating Power*

If actual $THDS_I$ value is available for equipment operating at specific power $P$ and for given voltage supply conditions $\bar{\boldsymbol{V}}^{\boldsymbol{H}}$, e.g. from the field measurement, this can be used for a more accurate calculation of the coefficient $k_{THD\_B}(P)$, while coefficient $k_{THD\_A}(P)$ is the same (determined from the tests with ideally sinusoidal supply voltage). If the available actual measured value is denoted as $THDS_{I\_actual}(P)$, it can be used instead of (7), i.e. instead of calculating the average of two $THDS_{I\_B}(P)$ values for WF2 and WF3:

$$THDS_{I\_B}(P) = THDS_{I\_actual}(P) - THDS_{I\_A}(P) \quad (14)$$

and then (8)-(12) can be used to calculate the corresponding resulting harmonic current emission.

The accuracy of the second modification approach, using actual $THDS_{I\_actual}(P)$ values from WF2 data to estimate $HAM_{\%\_est}(P)$ elements, is again checked by comparison with measurement-based $HAM_{\%\_meas}(P)$, calculated from a full set of HFM measurements for different operating powers of three PVIs. These results (Fig. 8) again demonstrate small errors.

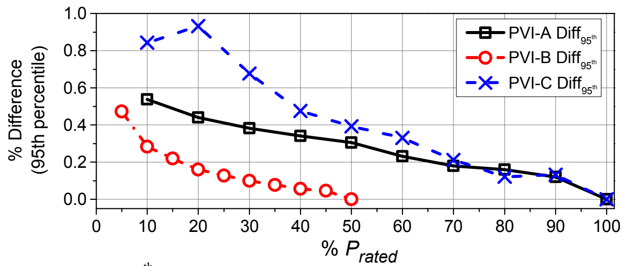


Fig. 8. The 95th percentile values of relative differences for estimated and measured $HAM_{\%}(P)$ elements (modification using actual $THDS_I$ values at PVI operating power).

## IV. Time-Domain Validation of HFMs

To validate accuracy of developed HFMs of three PVIs, the comparison of time-domain current waveforms for applied supply voltage waveforms WF2 and WF3 is given in Figs. 8-10. The following notation is used: measured instantaneous voltage waveforms, *v(t)*, and instantaneous current waveforms, *i(t)*, and related $THDS_I$ values are denoted with a subscript "Meas"; *i(t)* and related $THDS_I$ values reconstructed from measurement-based HFMs at corresponding operating powers are denoted as "M1"; *i(t)* and related $THDS_I$ values reconstructed from modified HFM using only PVI operating power are denoted as "M2"; *i(t)* and related $THDS_I$ values reconstructed from modified HFM using actual $THDS_I$ value at specific PVI operating power are denoted as "M3".

The results in Figs. 9-11 demonstrate not only a very good accuracy of the proposed approach for modelling PVIs power-dependent harmonic characteristics, but also its ability to correctly represent overall behavior of PVIs, as well as other types of power electronic devices with similar characteristics.

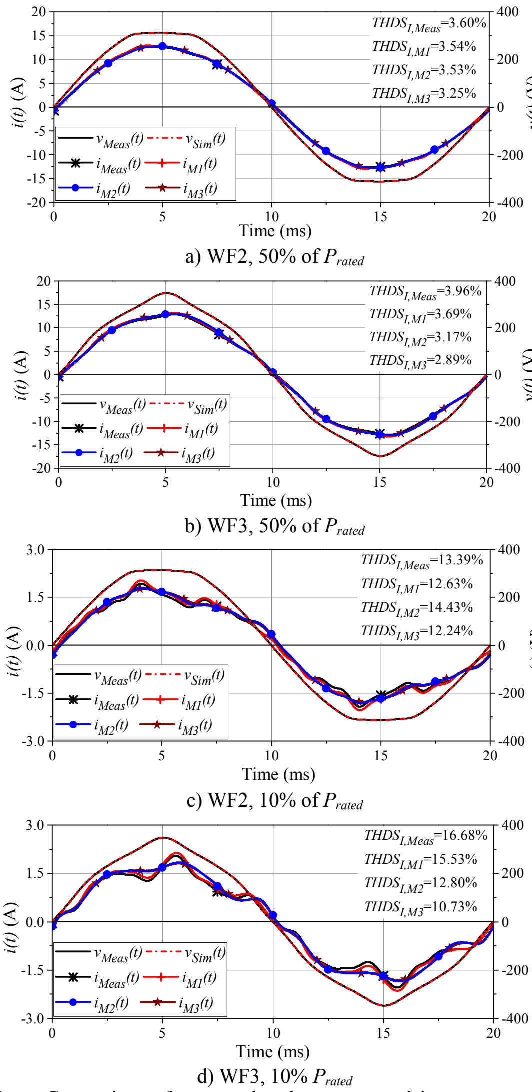


Fig. 9. Comparison of measured and reconstructed instantaneous current waveforms from different HFMs for PVI-A.

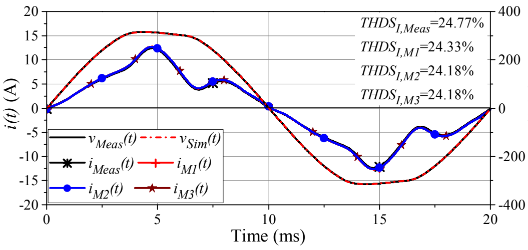


a) WF2, 50% of $P_{rated}$

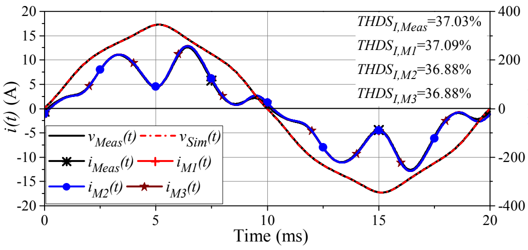


b) WF3, 50% of $P_{rated}$

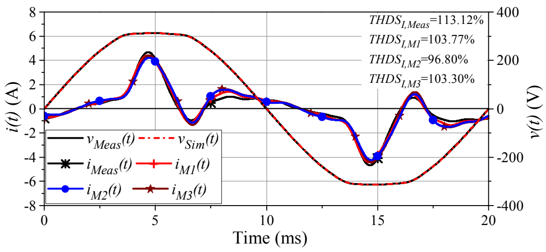


c) WF2, 10% of $P_{rated}$

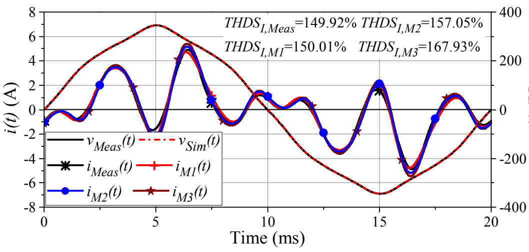


d) WF3, 10% of $P_{rated}$

Fig. 10. Comparison of measured and reconstructed instantaneous current waveforms from different HFMs for PVI-B.

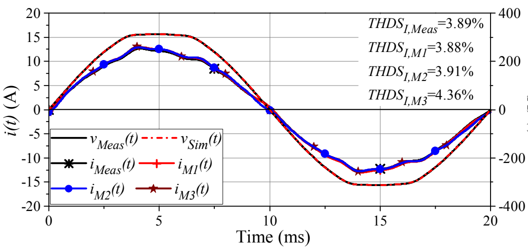


a) WF2, 50% of $P_{rated}$

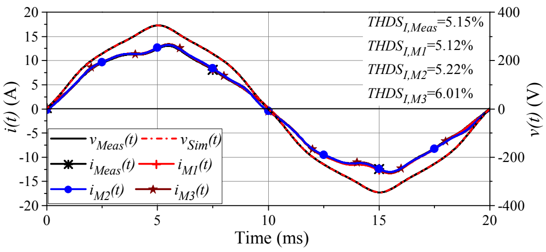


b) WF3, 50% of $P_{rated}$

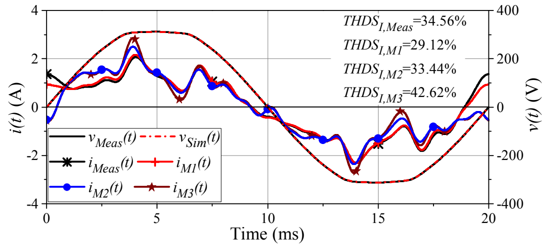


c)

WF2, 10% of $P_{rated}$

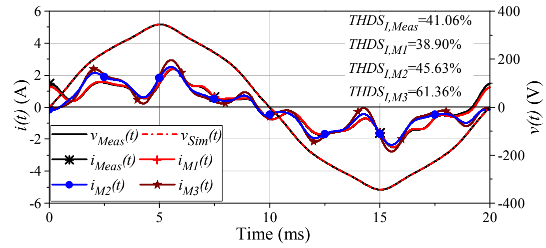


d) WF3, 10% of $P_{rated}$

Fig. 11. Comparison of measured and reconstructed instantaneous current waveforms from different HFMs for PVI-C.

## V. CONCLUSIONS

This paper, which is the first part of a two-part series on the development of aggregate FDMs of PVIs, introduces two simple modifications of HAMs in related measurement-based HFMs. This approach allows for the correct representation of power-dependent changes of PVIs harmonic characteristics with significantly reduced number of required tests. The presented approach is validated using comprehensive laboratory tests with three different PVIs, suggesting that it can correctly model not only harmonic characteristics, but also the overall behavior of PVIs. Part 2 paper provides further analysis of operation of parallel-connected PVI units and their aggregate HFM representations.

## REFERENCES

[1] R. Langella, A. Testa, J. Meyer, F. Möller, R. Stiegler and S. Z. Djokic, "Experimental-Based Evaluation of PV Inverter Harmonic and Interharmonic Distortion Due to Different Operating Conditions," *in IEEE Trans. on Instr. and Measurement*, vol. 65, no. 10, pp. 2221-2233, Oct. 2016.

[2] X. Xu, A. Collin, S. Djokic, R. Langella, A. Testa, J. Meyer and Friedemann Möller, "Harmonic emission of PV inverters under different voltage supply conditions and operating powers," *2016 17th Int. Conf. on Harm. and Quality of Power (ICHQP)*, Belo Horizonte, pp. 373-378, 2016.

[3] R. Langella, A. Testa, S. Z. Djokic, J. Meyer and M. Klatt, "On the interharmonic emission of PV inverters under different operating conditions," *17th Int. Conf. on Harm. and Quality of Power (ICHQP)*, Belo Horizonte, pp. 733-738, 2016.

[4] X. Xiao A. Collin, S. Djokic, S. Yanchenko, F. Möller, J. Meyer, R. Langella and A. Testa , "Analysis and Modelling of Power-Dependent Harmonic Characteristics of Modern PE Devices in LV Networks," *in IEEE Trans. on Power. Delivery*, vol. 32, no. 2, pp. 1014-1023, Apr. 2017.

[5] Sjef Cobben, Wil Kling, Johanna Myrzik, "The making and purpose of harmonic fingerprints", *19th Int. Conf. CIRED 2007*, Vienna, May 2007.

[6] A.S. Koch, J.M.A. Myrzik, T. Wiesner, L. Jendernalik: "Practical implementation of the Coupled Norton approach for nonlinear harmonic models", *18th Pow. Syst. Comp. Conf. (PSCC'14)*, August 2014.

[7] J. Meyer, S. Müller, P. Schegner, S. Z. Djokic, A. J. Collin and X. Xu, "Comparison of methods for modelling electric vehicle chargers for harmonic studies," *19th Pow. Syst. Comp. Conf. (PSCC)*, Genoa, 2016.

[8] *Voltage characteristics of electricity supplied by public electricity networks*, EN50160, July 2010.

[9] *Electromagnetic compatibility (EMC). Part 4-7: General guide on harmonics and interharmonics measurements for power supply systems and equipment connected thereto*, IEC Std. 61000-4-7. Ed. 2. 2009.